ACS OMEGA

http://pubs.acs.org/journal/acsodf

Article

Rapid and Robust Analysis of Coumatetralyl in Environmental Water and Human Urine Using a Portable Raman Spectrometer

Mengmeng Han, Juan Zhang, Haiyan Wei, Wei Zou, Mengping Zhang, Xiao Meng, Wenwen Chen, Hua Shao,* and Cuijuan Wang*

Cite This: *ACS Omega* 2023, 8, 12878−12885

Read Online

ACCESS | Metrics & More | Article Recommendations | Supporting Information

ABSTRACT: The widespread use and exposure of coumatetralyl (CMTT) has led to its accumulation in the environment and organisms, causing damage to ecosystems and adverse health effects in humans. Unfortunately, achieving fast detection of CMTT remains challenging. Herein, a rapid and robust surface-enhanced Raman spectroscopy (SERS) method was developed for rapid on-site detection of CMTT in environmental water and human urine. Clear trends were observed between the signal intensity and the logarithmic concentration of CMTT, ranging from 0.025 to 5.0 μg/mL with high reproducibility. The detection limits in water and human urine were as low as 1.53 and 13.71 ng/mL, respectively. The recoveries of CMTT for environmental water and urine samples were 90.2−98.2 and 82.0−87.5%, respectively, satisfactory for practical applications. The quantitative results of this approach were highly comparable to those obtained by high-performance liquid chromatography. Most importantly, it is cost-effective, operationally simple, and without a complicated sample preparation step. Detecting CMTT in water samples took only 5 min, and the detection of urine samples was completed within 8 min. This simple yet practical SERS approach offers a reliable application prospect for on-site CMTT detection in environmental water and point-of-care monitoring of poisoned patients.

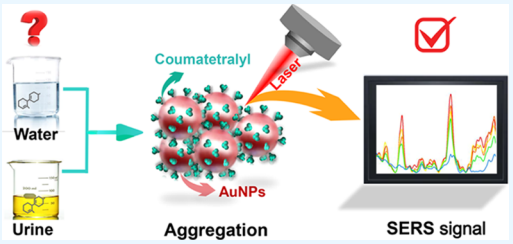

1. INTRODUCTION

The utilization of pesticides has greatly improved agricultural productivity and the quality of crops. Nevertheless, it also has brought inevitable harm to the ecosystem and human health due to the extensive applications.[1] Anticoagulant rodenticides (ARs), as a common pesticide, have been widely used to control symbiotic rodents.[2] Coumatetralyl (CMTT), an essential member of the AR family, has attracted public attention due to its persistence, bioaccumulation, and high toxicity.[3,4] The CMTT bait can be discharged directly into surface waters, agricultural irrigation, and livestock water,[5] causing the exposure of CMTT in aquatic environments.[4−6] CMTT has the potential for bioaccumulation and transfers through trophic webs,[7] adversely affecting the human health and the surrounding ecosystem.[8] In addition to environmental exposure, CMTT poisoning induced accidentally and by suicide has also become a significant global public health problem.[9−11] Since the bleeding symptoms caused by CMTT poisoning are similar to some medical diseases, it is easy to be misdiagnosed, resulting in delayed treatment and even irreparable health damage, which also brings great challenges to the detection of CMTT.[12] To date, there has been a lack of effective methods for rapid on-site detection of CMTT residues in environmental water and human biofluid, leading to the absence of monitoring data and underestimated exposure.[13]

Existing methods for detecting CMTT mainly include high-performance liquid chromatography (HPLC),[4] gas chromatography (GC),[14] thin layer chromatography,[15] HPLC−mass spectrometry (HPLC−MS),[16] and electrospray ionization-tandem mass spectrometry.[17] Although these methods are precise, they usually require complex and time-consuming preprocessing steps as well as skilled expertise, which greatly limit their field applications.[18,19] Currently, a rapid and user-friendly detection strategy for on-site detection and point-of-care monitoring of CMTT is desperately needed. Surface-enhanced Raman scattering (SERS) has multiple advantages over traditional analysis platforms, such as ultra-sensitive fingerprint acquisition, simple operation, fast readout speed, and low water interference.[20−22] These merits make SERS technology a promising analysis alternative and has been increasingly used in environmental analysis,[23] bio-medicine,[24,25] and food safety.[26] Recently, SERS has shown satisfactory performance in pesticide detection in soil[2] and vegetable samples.[27] SERS technology may significantly improve the efficiency of on-site detection of CMTT and provide timely essential information for environmental monitoring and poisoning treatment.

Received: January 1, 2023
Accepted: March 22, 2023
Published: March 30, 2023

https://doi.org/10.1021/acsomega.3c00005
ACS Omega 2023, 8, 12878−12885

Herein, a rapid and robust SERS method was developed for the on-site detection of CMTT in environmental water and human urine (Figure 1). Gold (Au) nanoparticles (Au NPs)

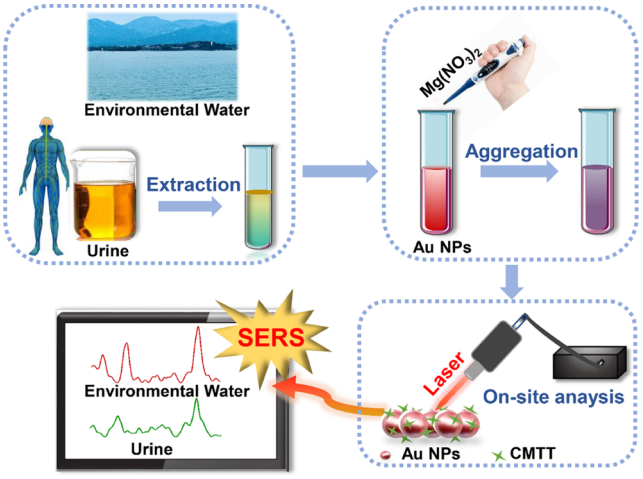

Figure 1. Schematic illustration for the SERS detection of coumatetralyl (CMTT) in environmental water and human urine.

were used as the substrate for enhancing the fingerprint signal of CMTT. The sensitivity of the technique was maximized by optimizing the aggregating conditions. A series of samples were analyzed using the standard addition method, and calibration curves were established with satisfactory recovery. This method combined the specificity of the SERS fingerprint, the portability of the portable Raman spectrometer, and the rapid readout of the spectra, thus realizing the specific, on-site, and rapid detection of CMTT in environmental water and complex biofluid. This SERS approach was applied to detect CMTT in real environmental water and urine. The whole analysis process could be completed within 5 min for water samples and less than 8 min for urine samples, which is more efficient than traditional methods. This simple yet practical SERS strategy has great potential for on-site environmental monitoring and point-of-care diagnosis.

2. MATERIALS AND METHODS

2.1. Chemicals and Reagents. CMTT (99.4%) was obtained from Dr. Ehrenstorfer (Beijing, China), purchased from a commercial source (CAS: 5836-29-3). Chloroauric acid ($HAuCl_4{\cdot}3H_2O$, 99.99%) and other reagents were purchased from Sinopharm Chemical Reagent Co., Ltd. (Shanghai, China). All the reagents were of analytical grade and used without further purification. The water used in the experiment was ultra-pure Milli-Q water (~18.2 MΩ·cm). Environmental samples were collected from the Black Tiger Spring in Jinan City, China. Urine samples were provided by healthy volunteers from the Shandong Academy of Occupational Health and Occupational Medicine.

2.2. Preparation of Au NPs. Au NPs were prepared by chemical reduction of chloroauric acid with trisodium citrate.[28] Briefly, 1 mL of 1% (w/v) chloroauric acid was added to 99 mL of deionized water, stirred at 600 rpm, and heated to boiling. Subsequently, 1 mL of a 1% (w/v) sodium citrate solution was added, followed by boiling for 35 min under vigorous stirring.

2.3. Instrumentation. SERS spectra were collected using a portable Raman spectrometer (QE Pro, Ocean Optics, USA) equipped with a 785 nm laser. The laser exposure time was set at 15 s, and the laser power was set at 300 mW (power density: 153 mw/mm^2). Optical absorption spectra of Au NPs were collected using a Shimadzu 2600 ultraviolet−visible light (UV−vis) spectrometer (Shimadzu Corp., Kyoto, Japan) at 25 °C. The uniformity and morphology were observed with a transmission electron microscope (TEM; JEM-CXII, JEOL Ltd., Tokyo, Japan) at 100 kV acceleration voltage.

2.4. Preparation of CMTT Solutions. A stock solution of CMTT with 2 mg/mL was prepared by dissolving solid CMTT in ethanol. Serial dilution of the stock solutions was then prepared with water or urine. A pooled human urine sample from 15 volunteers was used to exclude individual differences, given possible confounding factors in the experiment.[21,29−31] This study was approved by the ethics committee of the Shandong Academy of Occupational Health and Occupational Medicine (SDZFY-EC-H-2021-08) and conformed to the principles set out in the WMA Declaration of Helsinki.

2.5. Optimizing SERS Measurement. The aggregating effects of various salts [KCl, NaCl, $Mg(NO_3)_2$, $MgSO_4$, $CaCl_2$, and $Al(NO_3)_3$] on Au NPs were compared. First, 50 μL of CMTT solution (1 μg/mL) and 940 μL of Au NPs were mixed. Then, 10 μL of salt solution was added and mixed for 5 s to induce aggregation. The salt which induced optimal aggregation was selected. Moreover, the salt concentration (0.1, 0.25, 0.5, 1, and 2 M) was optimized. This strategy did not require pretreatment for water samples. For urine samples, the extraction effects of dichloromethane, *n*-hexane, ethyl acetate, acetonitrile, trichloroethane, and cyclohexane were compared. Different volumes of 1 M NaOH solution were used to adjust the alkalinity of the solution. A certain volume of 1 M NaOH and 0.3 g of NaCl were first added to a 1 mL spiked urine sample and mixed thoroughly. The solution was then mixed with 2 mL of organic solvents, and the organic layer was taken for SERS detection.

3. RESULTS AND DISCUSSION

3.1. Characterization of Au NPs. TEM results showed that the Au NPs were 45−60 nm in size and had a uniform shape (Figure 2a). The absorption peak of Au NPs solution was located at 522 nm (Figure 2b). After adding 50 μL of 1 μg/mL CMTT to the solution, no apparent changes were observed. In contrast, the addition of 10 μL of 0.5 M $Mg(NO_3)_2$ resulted in a significant decrease in absorption strength, accompanied by a change in color from brick red to purplish gray (Figure 2b), indicating aggregation.[32] Figure 2c further displays that the particle gaps became smaller and fused, and the dispersed nanoparticles in the colloidal solution agglomerated. The Raman and SERS signals corresponding to the UV−vis spectra are shown in Figure 2d.

3.2. Raman Characterization of CMTT. Reference Raman spectra of solid CMTT and SERS spectra of aqueous CMTT (1 μg/mL) were collected using a portable Raman spectrometer. Since CMTT contains an active hydroxyl functional group (inset in Figure 2e), it can produce derivatives of various structures. Lone pairs of electrons in the CMTT structure can coordinate with metal ions and participate in hydrogen bonds. Thus, the characteristic shift of CMTT between solid and aqueous solutions may change slightly (Figure 2e). In an aqueous solution, the two distinct Raman spectral bands of the solid standard at 670 and 1007 cm^{-1} were shifted to 665 and 995 cm^{-1}, respectively. The peak at 665 cm^{-1} is attributed to C−C−C in the aromatic ring.[33] Aromatic C−H vibrations cause the characteristic Raman peak at 995 cm^{-1}.[34] In addition, the band at 557 cm^{-1} is mainly associated with the phenyl ring breathing

https://doi.org/10.1021/acsomega.3c00005
ACS Omega 2023, 8, 12878−12885

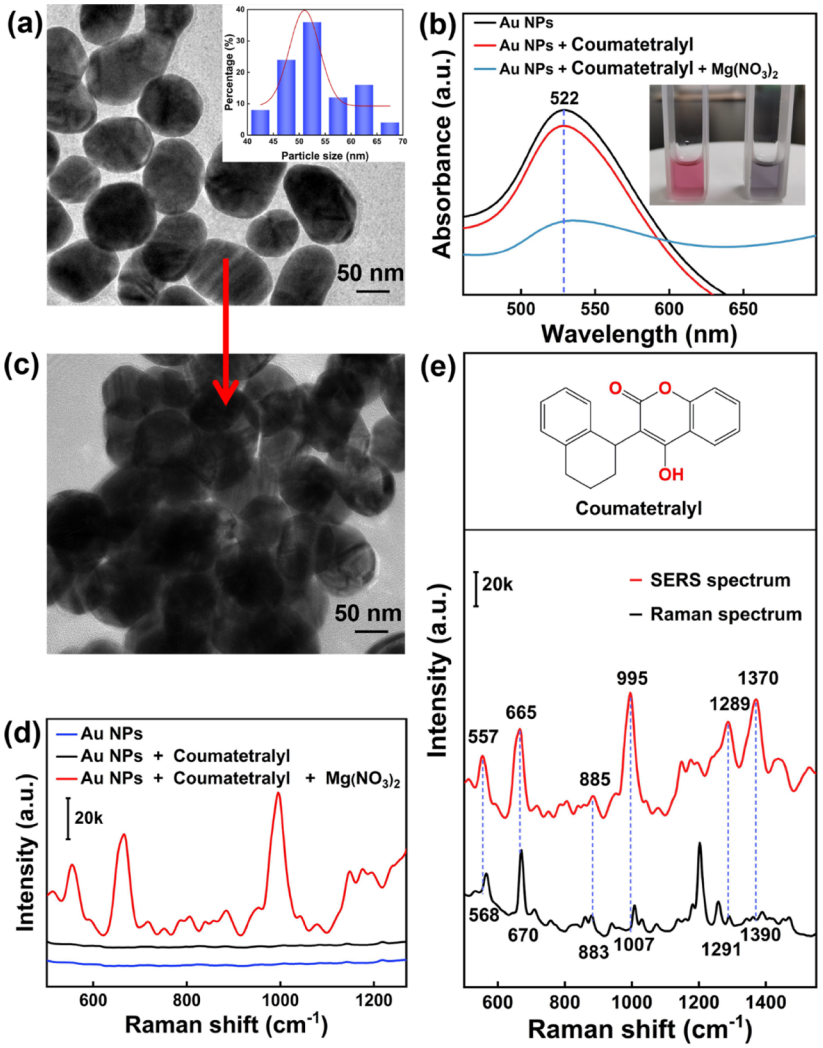

Figure 2. TEM images of Au NPs before (a) and after aggregation (c); (b) UV−vis spectra of colloidal Au NPs, Au NPs mixed with 1 μg/mL CMTT and aggregated Au NPs after adding 10 μL of 0.5 M $Mg(NO_3)_2$. The inner part shows the color change; (d) SERS spectrum of the solutions corresponding to (b); (e) The chemical structure of CMTT, the Raman spectrum of solid standard CMTT, and the SERS spectrum of CMTT solution.

mode,[35] the band at 885 cm^{-1} is assigned as CH_2 mode,[36] and the 1289 and 1370 cm^{-1} mainly due to C−H bending mode.[35] In this work, the SERS response band at 995 cm^{-1} was selected as the quantitative signal.

3.3. Optimization of Aggregation Conditions. The performance of colloidal substrates is usually affected by the degree of aggregation.[37,38] In this study, the SERS intensity of 1 μg/mL CMTT produced by six aggregating salts with the same concentration (0.5 M) was first compared. The enhancing effects were in the order of $Mg(NO_3)_2$ > $MgSO_4$ > $Al(NO_3)_3$ > $CaCl_2$ > NaCl > KCl (Figure 3a). Divalent and trivalent cations have been proven more effective in inducing aggregation than monovalent cations.[39] An Au NPs colloidal solution generally remains stable because the particles have the same charge on the surface and repel each other. Adding salt causes the heteros distributed in the diffuse layer to be squeezed into the adsorption layer.[40] Reduced zeta potential and the decreasing repulsive force between the particles can lead to aggregation[41,42] and the generation of hot spots, resulting in surface-enhanced resonance.[43,44] Thus, in this study, $Mg(NO_3)_2$ was selected as the aggregation agent. It is also worth noting that insufficient or excessive aggregation tends to reduce the number of hot spots.[45] Therefore, the concentrations of $Mg(NO_3)_2$ (0.1, 0.25, 0.5, 1, and 2 M) were next selected. From Figure 3b, the strongest SERS signal was induced by 0.5 M $Mg(NO_3)_2$, and thus was used as the aggregating agent.[46]

Moreover, the effects of aggregating time on SERS intensity in water (Figure 3c,d) and urine (Figure 3e,f) were examined by recording a continuous SERS signal. Overall, the signal remained relatively stable within 30 min. Here, 5 min was selected as the aggregating time, considering the detection efficiency and sensitivity. Under the optimized conditions, the average enhancement factor was calculated to be 1.29×10^6.

3.4. SERS Analysis of CMTT in Water. As shown in Figure 4a, the intensity of the 665 and 995 cm^{-1} peaks increased with a high concentration of CMTT in a standard aqueous solution. Since the SERS signal intensity at 995 cm^{-1} is stronger and the SERS peak is easier to observe, the SERS response band at 995 cm^{-1} is selected as the quantitative signal in this study. It is worth noting that there were two bands located around 995 cm^{-1}. In order to better readout the SERS signal intensity, sub-peak fitting was carried out. Figure 4b illustrates the quantitative calibration curve of the SERS intensity against the logarithmic concentration. In the range of 0.025−5 μg/mL, the response

https://doi.org/10.1021/acsomega.3c00005
ACS Omega 2023, 8, 12878−12885

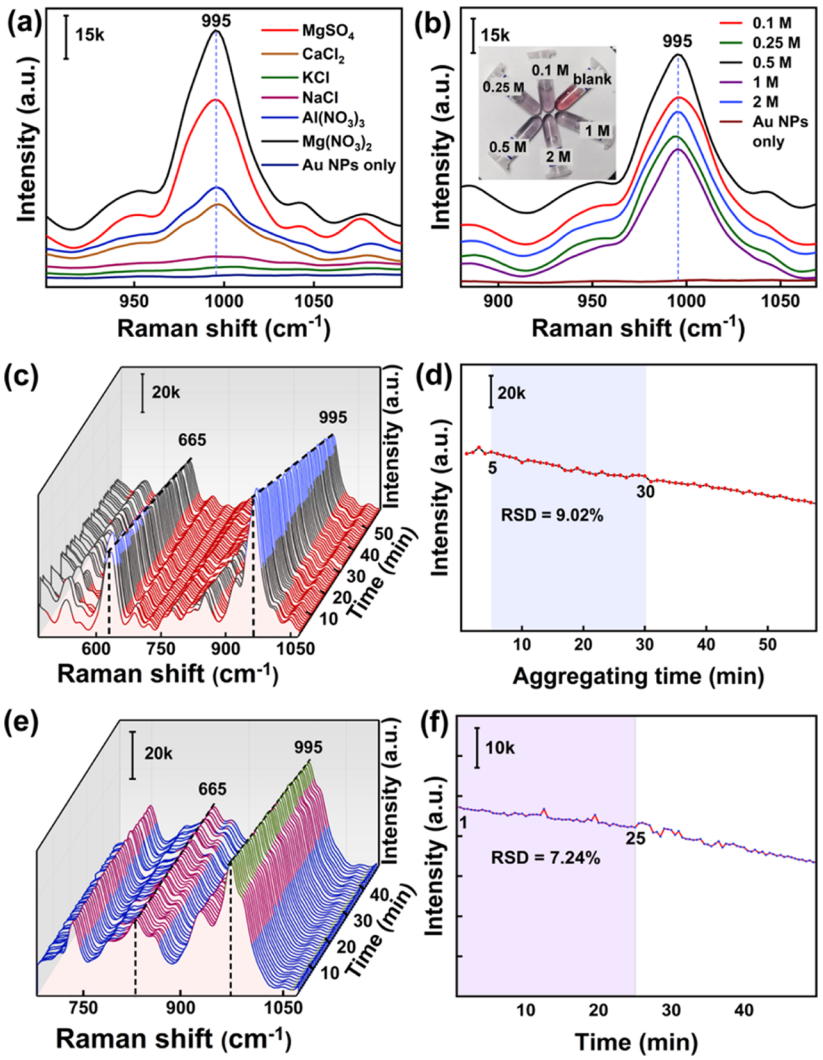

Figure 3. Effects of various types (a) and concentrations (b) of aggregating salts on SERS signal intensity at 995 cm^{-1}. The inset shows the color change of solutions induced by different concentrations of $Mg(NO_3)_2$. Temporal evolution of the SERS spectra of CMTT in water (c) and urine (e); Temporal evolution of the SERS intensity of 995 cm^{-1} peaks in water (d) and urine (f).

showed a clear linear dependence (R^2 = 0.987), which met the requirements of quantitative detection. To verify the feasibility and utility of the proposed SERS method, CMTT in spiked real environmental water was detected. The fingerprint signal of CMTT was collected within 5 min without any pretreatment steps. The SERS signal intensity at 995 cm^{-1} increased with higher CMTT concentrations, similar to the trend in standard aqueous solutions (Figure S1).

The long-term stability and reproducibility of SERS substrates are critical analytical performance parameters. Two concentrations of CMTT spiked in water samples (0.05 and 1 μg/mL) were analyzed on different days in 21 parallel experiments using the same substrate batch. Figure 4c shows that the corresponding relative standard deviations (RSDs) were 6.81 and 9% for 1 and 0.05 μg/mL, respectively. Furthermore, the intraday and interday precision were evaluated using eight batches fabricated on 8 days or the same day, and the RSDs were within 10% (Figure 4d). These results indicate sufficient long-term stability and reproducibility of this proposed method for practical applications.

3.5. SERS Analysis of CMTT in Urine. The complex matrix in urine involved intermolecular, coordination, or hydrogen bonding interactions, which might compete with CMTT for binding sites on Au NPs, thus affecting detection sensitivity.[39] Thus, the separation of CMTT from the urine matrix was optimized.

The effect of pH on extraction efficiency was first studied. Figure S2 shows that the extraction efficiency in an alkaline environment was much higher than in an acidic environment. The SERS signal was the strongest when pH was 12 (Figure S3a). This effect might be attributed to the protonation of hydroxyl groups on the molecule under acidic conditions, resulting in CMTT being charged in an aqueous solution. Under an alkaline condition, in contrast, CMTT existed in deprotonated form, which yielded it more easily extracted into the organic solvent layer. Meanwhile, CMTT has a stronger affinity to the Au surface under alkaline conditions, decreasing the colloidal stability of Au NPs and thereby accelerating the formation of Au NP aggregates.[28]

Second, the extraction performances of dichloromethane, *n*-hexane, ethyl acetate, acetonitrile, trichloroethane, and cyclohexane were investigated. Due to its hydrophobicity, CMTT can be separated and enriched by partitioning into organic solvents. Ethyl acetate was observed to provide the strongest SERS signal.

https://doi.org/10.1021/acsomega.3c00005
ACS Omega 2023, 8, 12878−12885

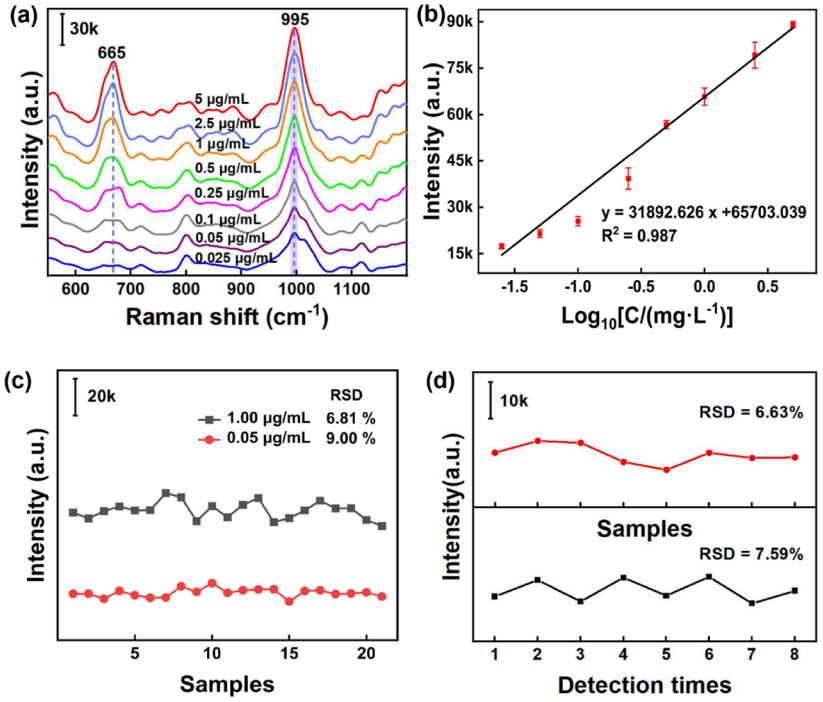

Figure 4. (a) SERS spectra of increasing concentrations of CMTT in a standard aqueous solution. (b) Plot of the SERS peak at 995 cm^{-1} versus the log of aqueous CMTT concentrations after deconvolution. (c) SERS intensity at 995 cm^{-1} of 1 μg/mL (black line) and 0.05 (red line) μg/mL CMTT acquired over 21 days using the same batch of Au NPs. (d) SERS intensity at 995 cm^{-1} using eight batches of Au NPs prepared on 8 days (black line) and on the same day (red line).

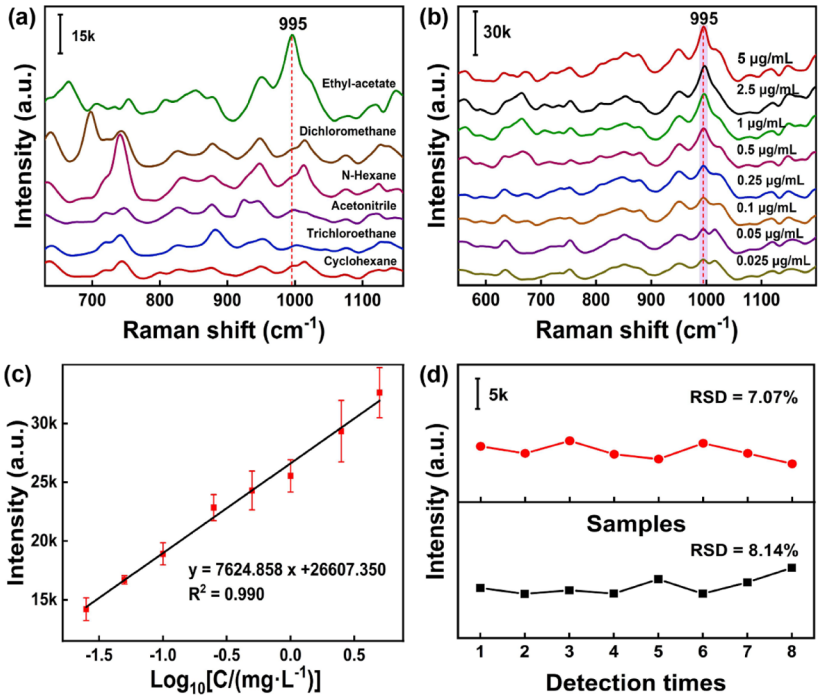

Figure 5. (a) Comparison of performance of different organic solvents for the extraction of CMTT from the urine. (b) SERS spectra stacked in the order of increasing concentration of CMTT in urine. (c) Plot of the SERS peak at 995 cm^{-1} versus the log concentration of urinary CMTT after deconvolution. (d) SERS intensity at 995 cm^{-1} of CMTT (0.1 μg/mL) in urine using eight batches of Au NPs prepared on 8 days (black line) and the same day (red line).

It may be due to the good solubility of CMTT in ethyl acetate compared with other organic extractants and the better stratification of the organic and aqueous phases under the same conditions. Meanwhile, ethyl acetate was less toxic. Thus, ethyl acetate was selected as the extraction solvent (Figure 5a). The urine-to-ethyl acetate ratio was determined to be 1/2 (v/v) (Figure S3b). The separation process was time-saving and operator-friendly, suitable for field detection.

Under optimal conditions, SERS spectral bands of various CMTT concentrations were recorded (Figure 5b). After

https://doi.org/10.1021/acsomega.3c00005
ACS Omega 2023, 8, 12878−12885

deconvolution, Figure 5c shows a clear linear relationship between log concentrations of urinary CMTT and the SERS intensity of 995 cm^{-1} (R^2 = 0.990). RSDs of intraday and interday were 8.14 and 7.07%, respectively (Figure 5d), indicating satisfactory analysis performance.

3.6. Recoveries and Detection Limits. To further estimate the applicability of this SERS method, the recoveries of CMTT in real environmental water and human urine were investigated. The average recoveries were 90.2−98.2% in water (n = 8) and 82.0−87.5% in urine (n = 6), respectively (Table 1 and Figure S4). The LODs were calculated to be 1.53 ng/mL in water and 13.71 ng/mL in human urine using a method from a previous study,[28] which are sufficient to meet the needs of route detection. These results suggested that the proposed method is a promising strategy for on-site detecting CMTT in environmental water and point-of-care monitoring.

Table 1. Average Recoveries of Different CMTT Concentrations in Spiked Environmental Water and Human Urine

added (μg/mL)	found ± SD (μg/mL)	recovery (%)	RSD (%)
	Water——		
0.50	0.48 ± 0.12	96.4	6.40
1.00	0.90 ± 0.12	90.2	2.96
2.50	2.46 ± 0.36	98.2	2.94
	Urine——		
0.25	0.22 ± 0.04	87.4	6.08
1.00	0.88 ± 0.15	87.5	3.73
5.00	4.10 ± 1.47	82.0	6.21

3.7. HPLC Measurements for Benchmarking. An HPLC method was implemented to confirm the accuracy of this SERS-based method. As shown in Figure 6a, the results obtained by these two methods exhibited good agreement (R^2 = 0.997). These results further confirm the reliability and accuracy of the proposed method.

3.8. Specificity of This SERS System for CMTT Detection. There might be other kinds of confounding pesticide residues in environmental water and potential coexisting biological substances in human urine. Herein, the specificity for CMTT was evaluated by conducting SERS detection of several potential coexisting pesticides (brodifacoum, difenacoum, diquat, and thiram) and biological substances (creatinine and uric acid). The fingerprint information of a compound is obtained by Raman spectroscopy according to the vibration of its chemical bond spatial structure, to generate SERS response at different Raman shifts of the chromatography. Since the spatial composition of CMTT differs from that of other chemicals, the fingerprints are also significantly different, which results in excellent selectivity. According to Figure 6b, none of these substances showed an obvious SERS signal at 995 cm^{-1} shift, demonstrating the high selectivity of this assay.

A comparison between the proposed and traditional methods is shown in Table S1. Traditional detection methods, such as HPLC, GC, and LC-MS/MS, have limited application in field detection, requiring multiple large-sized instruments, multistep operations, and professional technicians.[47] On the contrary, our proposed assay is rapid, low-cost, and easy to operate, thus having outstanding advantages in on-site detection. In addition, it has great potential as a point-of-care device in clinical diagnosis due to the portable instrument.

4. CONCLUSIONS

In summary, a rapid on-site SERS strategy was developed using Au NPs as the substrate for qualitative and quantitative CMTT determination in environmental water and human urine. SERS signals were collected directly using a portable Raman spectrometer, which is fast, economical, and practical. The whole process can be completed in 5 min for environmental water and 8 min for human urine samples, with satisfactory LODs and recovery rates. The quantitative results of this SERS assay were compared with those determined using an HPLC method, and the results of these two methods were highly consistent. In brief, the characteristics of this approach of sensitivity, reproducibility, and stability provided a promising route for the identification and quantification of CMTT. We believe this efficient SERS method has great potential in environmental monitoring and point-of-care diagnosis of poisoned patients.

■ ASSOCIATED CONTENT

Supporting Information

The Supporting Information is available free of charge at https://pubs.acs.org/doi/10.1021/acsomega.3c00005.

SERS signals of different concentrations of CMTT; influence of pH on SERS signal of CMTT in human urine; influence of NaOH volume on SERS signal of urine; SERS intensity of eight water samples with various concentrations of CMTT; and comparison of various available CMTT detection methods (PDF)

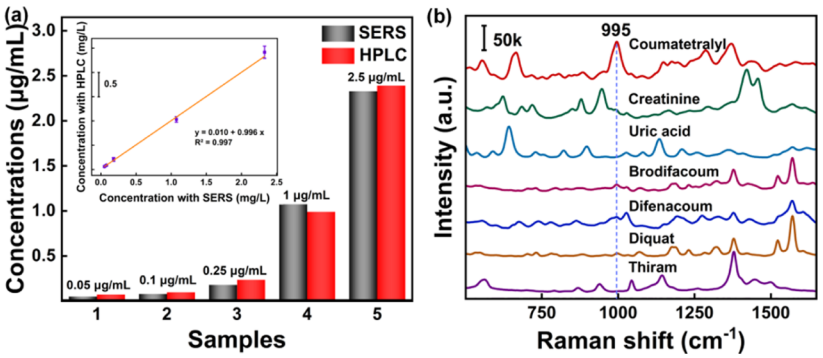

Figure 6. (a) Comparison of two methods for detecting CMTT in urine, the inner part displays a calibration plot of the concentration values obtained by SERS versus those analyzed by an HPLC method. (b) SERS spectra of possible coexisting pesticides and biological substances.

https://doi.org/10.1021/acsomega.3c00005
ACS Omega 2023, 8, 12878−12885

AUTHOR INFORMATION

Corresponding Authors

Hua Shao − *Physical and Chemical Laboratory, Shandong Academy of Occupational Health and Occupational Medicine, Shandong First Medical University & Shandong Academy of Medical Sciences, Jinan 250000, China*; Email: chinashaohua5888@163.com

Cuijuan Wang − *Physical and Chemical Laboratory, Shandong Academy of Occupational Health and Occupational Medicine, Shandong First Medical University & Shandong Academy of Medical Sciences, Jinan 250000, China*; orcid.org/0000-0002-4839-274X; Email: wangcuijuan@sdfmu.edu.cn

Authors

Mengmeng Han − *Physical and Chemical Laboratory, Shandong Academy of Occupational Health and Occupational Medicine, Shandong First Medical University & Shandong Academy of Medical Sciences, Jinan 250000, China*

Juan Zhang − *Physical and Chemical Laboratory, Shandong Academy of Occupational Health and Occupational Medicine, Shandong First Medical University & Shandong Academy of Medical Sciences, Jinan 250000, China*

Haiyan Wei − *Physical and Chemical Laboratory, Shandong Academy of Occupational Health and Occupational Medicine, Shandong First Medical University & Shandong Academy of Medical Sciences, Jinan 250000, China*

Wei Zou − *Physical and Chemical Laboratory, Shandong Academy of Occupational Health and Occupational Medicine, Shandong First Medical University & Shandong Academy of Medical Sciences, Jinan 250000, China*

Mengping Zhang − *Physical and Chemical Laboratory, Shandong Academy of Occupational Health and Occupational Medicine, Shandong First Medical University & Shandong Academy of Medical Sciences, Jinan 250000, China*

Xiao Meng − *Physical and Chemical Laboratory, Shandong Academy of Occupational Health and Occupational Medicine, Shandong First Medical University & Shandong Academy of Medical Sciences, Jinan 250000, China*

Wenwen Chen − *Physical and Chemical Laboratory, Shandong Academy of Occupational Health and Occupational Medicine, Shandong First Medical University & Shandong Academy of Medical Sciences, Jinan 250000, China*

Complete contact information is available at: https://pubs.acs.org/10.1021/acsomega.3c00005

Author Contributions

M.H.: writing—original draft, validation, software. J.Z.: formal analysis, visualization. H.W.: methodology, investigation. W.Z.: validation. M.Z.: data curation. X.M. and W.C.: methodology. H.S.: project administration, funding acquisition. C.W.: conceptualization, writing—review and editing, supervision. M.H. and J.Z. contributed equally to this work and should be considered co-first authors.

Notes

The authors declare no competing financial interest.

Human urine trials were performed in accordance with a permit issued to the Ethics Review Committee of Shandong Institute of Occupational Health and Disease Prevention: SDZFY-EC-H-2021-08.

ACKNOWLEDGMENTS

This project was supported by the National Science Foundation of China (no. 81872575); Shandong Provincial Medical and Health Science and Technology Development Plan (nos. 202112070425 and 202212010448); Shandong Provincial Traditional Chinese Medicine Science and Technology Project (no. 2021M152); Clinical Medical Science and Technology Innovation Plan of Jinan (202225062); Key Research and Development Plan of Shandong Province (no. 2017GSF18186); and the Academic Promotion Program of Shandong First Medical University (no. 2019QL001).

REFERENCES

(1) Bernat, A.; Samiwala, M.; Albo, J.; Jiang, X.; Rao, Q. Challenges in SERS-based pesticide detection and plausible solutions. *J. Agric. Food Chem.* **2019**, *67*, 12341−12347.

(2) Gong, T.; Huang, Y.; Wei, Z.; Huang, W.; Wei, X.; Zhang, X. Magnetic assembled 3D SERS substrate for sensitive detection of pesticide residue in soil. *Nanotechnology* **2020**, *31*, 205501.

(3) Walther, B.; Ennen, H.; Geduhn, A.; Schlötelburg, A.; Klemann, N.; Endepols, S.; Schenke, D.; Jacob, J. Effects of anticoagulant rodenticide poisoning on spatial behavior of farm dwelling Norway rats. *Sci. Total Environ.* **2021**, *787*, 147520.

(4) Regnery, J.; Friesen, A.; Geduhn, A.; Göckener, B.; Kotthoff, M.; Parrhysius, P.; Petersohn, E.; Reifferscheid, G.; Schmolz, E.; Schulz, R. S.; et al. Rating the risks of anticoagulant rodenticides in the aquatic environment: a review. *Environ. Chem. Lett.* **2018**, *17*, 215−240.

(5) Kotthoff, M.; Rüdel, H.; Jürling, H.; Severin, K.; Hennecke, S.; Friesen, A.; Koschorreck, J. First evidence of anticoagulant rodenticides in fish and suspended particulate matter: spatial and temporal distribution in German freshwater aquatic systems. *Environ. Sci. Pollut. Res.* **2019**, *26*, 7315−7325.

(6) Deknock, A.; De Troyer, N.; Houbraken, M.; Dominguez-Granda, L.; Nolivos, I.; Van Echelpoel, W.; Forio, M. A. E.; Spanoghe, P.; Goethals, P. Distribution of agricultural pesticides in the freshwater environment of the Guayas river basin (Ecuador). *Sci. Total Environ.* **2019**, *646*, 996−1008.

(7) Acosta-Dacal, A.; Rial-Berriel, C.; Diaz-Diaz, R.; Bernal-Suarez, M.; Zumbado, M.; Henriquez-Hernandez, L.; Luzardo, O. P. An Easy Procedure to Quantify Anticoagulant Rodenticides and Pharmaceutical Active Compounds in Soils. *Toxics* **2021**, *9*, 83.

(8) Walther, B.; Geduhn, A.; Schenke, D.; Schlötelburg, A.; Jacob, J. Baiting location affects anticoagulant rodenticide exposure of non-target small mammals on farms. *Pest Manag. Sci.* **2021**, *77*, 611−619.

(9) Rattner, B. A.; Harvey, J. J. Challenges in the interpretation of anticoagulant rodenticide residues and toxicity in predatory and scavenging birds. *Pest Manag. Sci* **2021**, *77*, 604−610.

(10) Gopalakrishnan, S.; Kandasamy, S.; Iyyadurai, R. *Rodenticide Poisoning: Critical Appraisal of Patients at a Tertiary Care Center*; Indian Journal of Critical Care Medicine: Peer-reviewed Official Publication of Indian SCCM, 2020; Vol. *24*, pp 295−298.

(11) Rahman, N. A.; Das, S.; Chaudhari, V. A.; Nandagopal, S.; Badhe, B. Blending of rodenticide and battery acid − a rare and fatal suicide mix. *Egyptian JFS* **2017**, *7*, 8.

(12) Chen, Y.; Liu, H.; Tian, Y.; Du, Y.; Ma, Y.; Zeng, S.; Gu, C.; Jiang, T.; Zhou, J. In Situ Recyclable Surface-Enhanced Raman Scattering-Based Detection of Multicomponent Pesticide Residues on Fruits and Vegetables by the Flower-like MoS2@Ag Hybrid Substrate. *ACS Appl. Mater. Interfaces* **2020**, *12*, 14386−14399.

(13) Regnery, J.; Parrhysius, P.; Schulz, R. S.; Möhlenkamp, C.; Buchmeier, G.; Reifferscheid, G.; Brinke, M. Wastewater-borne exposure of limnic fish to anticoagulant rodenticides. *Water Res.* **2019**, *167*, 115090.

(14) Bergrath, S.; Castillo-Vargas, J. S.; Koc, N. J.; Haake, H.; Graeven, U. Suspected seizure—survival of a lethal dose of the rodenticide alpha-chloralose. *Der Anaesthesist* **2019**, *68*, 843−847.

(15) De Bairros, A. V.; Dias, D.; Bezerra, A.; Wagner, R.; Klein, B.; Kommers, G.; Stefanon, E.; Miguel Pego, A. An analytical strategy for the identification of carbamates, toxic alkaloids, phenobarbital and warfarin in stomach contents from suspected poisoned animals by thin-layer chromatography/ultraviolet detection. *Toxicol. Mech. Methods* **2019**, *29*, 518−530.
(16) Elmeros, M.; Lassen, P.; Bossi, R.; Topping, C. J. Exposure of stone marten (Martes foina) and polecat (Mustela putorius) to anticoagulant rodenticides: Effects of regulatory restrictions of rodenticide use. *Sci. Total Environ.* **2018**, *612*, 1358−1364.
(17) Seljetun, K. O.; Sandvik, M.; Vindenes, V.; Eliassen, E.; Øiestad, E. L.; Madslien, K.; Moe, L. Comparison of anticoagulant rodenticide concentrations in liver and feces from apparently healthy red foxes. *J. Vet. Diagn. Invest.* **2020**, *32*, 560−564.
(18) Okoniewski, R.; Neely, S.; Denn, M.; Djatsa, A.; Tran, B. N. Rapid method for the detection of rodenticides in contaminated foods. *J. Chromatogr., B, J Chromatogr B Analyt Technol Biomed Life Sci* **2021**, *1186*, 123005.
(19) Valverde, I.; Espín, S.; Gómez-Ramírez, P.; Navas, I.; María-Mojica, P.; Sánchez-Virosta, P.; Jiménez, P.; Torres-Chaparro, M. Y.; García-Fernández, A. J. Wildlife poisoning: a novel scoring system and review of analytical methods for anticoagulant rodenticide determination. *Ecotoxicology* **2021**, *30*, 767−782.
(20) Fang, W.; Zhang, B.; Han, F. Y.; Qin, Z. N.; Feng, Y. Q.; Hu, J. M.; Shen, A. G. On-Site and Quantitative Detection of Trace Methamphetamine in Urine/Serum Samples with a Surface-Enhanced Raman Scattering-Active Microcavity and Rapid Pretreatment Device. *Anal. Chem.* **2020**, *92*, 13539−13549.
(21) Jiang, J.; Xu, L.; Zhang, Y.; Ma, J.; Gu, C.; Zhou, X.; Wei, G.; Jiang, T. Quantitative and recyclable SERS detection induced by tunable Raman internal standard from embedded silicon nanoparticles. *Sens. Actuators, B* **2022**, *366*, 131989.
(22) Li, D.; Xia, L.; Zhou, Q.; Wang, L.; Chen, D.; Gao, X.; Li, Y. Label-Free Detection of miRNA Using Surface-Enhanced Raman Spectroscopy. *Anal. Chem.* **2020**, *92*, 12769−12773.
(23) Tian, C.; Zhao, L.; Zhu, J.; Zhang, S. Ultrasensitive detection of trace Hg2+ by SERS aptasensor based on dual recycling amplification in water environment. *J. Hazard. Mater.* **2021**, *416*, 126251.
(24) Wang, G.; Hao, C.; Ma, W.; Qu, A.; Chen, C.; Xu, J.; Xu, C.; Kuang, H.; Xu, L.; Xu, L.; Kuang, H.; Xu, L. G. Chiral Plasmonic Triangular Nanorings with SERS Activity for Ultrasensitive Detection of Amyloid Proteins in Alzheimers Disease. *Adv. Mater.* **2021**, *33*, 2102337.
(25) Lu, X.; Ren, W.; Hu, C.; Liu, C.; Li, Z. Plasmon-Enhanced Surface-Enhanced Raman Scattering Mapping Concentrated on a Single Bead for Ultrasensitive and Multiplexed Immunoassay. *Anal. Chem.* **2020**, *92*, 12387−12393.
(26) He, X.; Yang, S.; Xu, T.; Song, Y.; Zhang, X. Microdroplet-captured tapes for rapid sampling and SERS detection of food contaminants. *Biosens. Bioelectron.* **2020**, *152*, 112013.
(27) Chen, J.; Huang, M.; Kong, L.; Lin, M. Jellylike flexible nanocellulose SERS substrate for rapid in-situ non-invasive pesticide detection in fruits/vegetables. *Carbohydr. Polym.* **2019**, *205*, 596−600.
(28) Zhang, M.; Pan, J.; Xu, X.; Fu, G.; Zhang, L.; Sun, P.; Yan, X.; Liu, F.; Wang, C.; Liu, X.; et al. Gold-Trisoctahedra-Coated Capillary-Based SERS Platform for Microsampling and Sensitive Detection of Trace Fentanyl. *Anal. Chem.* **2022**, *94*, 4850−4858.
(29) Zhu, W.; Wen, B. Y.; Jie, L. J.; Tian, X. D.; Yang, Z. L.; Radjenovic, P. M.; Luo, S. Y.; Tian, Z. Q.; Li, J. F. Rapid and low-cost quantitative detection of creatinine in human urine with a portable Raman spectrometer. *Biosens. Bioelectron.* **2020**, *154*, 112067.
(30) Westley, C.; Xu, Y.; Thilaganathan, B.; Carnell, A. J.; Turner, N. J.; Goodacre, R. Absolute Quantification of Uric Acid in Human Urine Using Surface Enhanced Raman Scattering with the Standard Addition Method. *Anal. Chem.* **2017**, *89*, 2472−2477.
(31) Kao, Y. C.; Han, X.; Lee, Y. H.; Lee, H. K.; Phan-Quang, G. C.; Lay, C. L.; Sim, H. Y. F.; Phua, V. J. X.; Ng, L. S.; Ku, C. W.; Tan, T. C.; Phang, I. Y.; Tan, N. S.; Ling, X. Y. Multiplex Surface-Enhanced Raman Scattering Identification and Quantification of Urine Metabolites in Patient Samples within 30 min. *ACS Nano* **2020**, *14*, 2542−2552.
(32) Mostowtt, T.; Munoz, J.; McCord, B. An evaluation of monovalent, divalent, and trivalent cations as aggregating agents for surface-enhanced Raman spectroscopy (SERS) analysis of synthetic cannabinoids. *Analyst* **2019**, *144*, 6404−6414.
(33) Hidi, I. J.; Jahn, M.; Weber, K.; Bocklitz, T.; Pletz, M. W.; Cialla-May, D.; Popp, J. LoC-SERS Combined with the Standard Addition Method: Toward the Quantification of Nitroxoline in Spiked Human Urine Samples. *Anal. Chem.* **2016**, *88*, 9173.
(34) Zhang, Y.; Li, L.; Gao, Y.; Wang, X.; Sun, L.; Ji, W.; Ozaki, Y. Nitrosonaphthol reaction-assisted SERS assay for selective determination of 5-hydroxyindole-3-acetic acid in human urine. *Anal. Chim. Acta* **2020**, *1134*, 34.
(35) Mary, Y. S.; Raju, K.; Yildiz, I.; Temiz-Arpaci, O.; Nogueira, H. I.; Granadeiro, C. M.; Van Alsenoy, C. V. FT-IR, FT-Raman, SERS and computational study of 5-ethylsulphonyl-2-(o-chlorobenzyl)-benzoxazole. *Spectrochim. Acta Mol. Biomol. Spectrosc.* **2012**, *96*, 617−625.
(36) Raj, A.; Sheena Mary, Y.; Yohannan Panicker, C.; Varghese, H. T.; Raju, K. IR, Raman, SERS and computational study of 2-(benzylsulfanyl)-3,5-dinitrobenzoic acid. *Spectrochim. Acta Mol. Biomol. Spectrosc.* **2013**, *113*, 28−36.
(37) Chan, M. Y.; Leng, W.; Vikesland, P. J. Surface-Enhanced Raman Spectroscopy Characterization of Salt-Induced Aggregation of Gold Nanoparticles. *ChemPhysChem* **2017**, *19*, 24−28.
(38) Subaihi, A.; Almanqur, L.; Muhamadali, H.; AlMasoud, N.; Ellis, D. I.; Trivedi, D. K.; Hollywood, K. A.; Xu, Y.; Goodacre, R. Rapid, Accurate, and Quantitative Detection of Propranolol in Multiple Human Biofluids via Surface-Enhanced Raman Scattering. *Anal. Chem.* **2016**, *88*, 10884−10892.
(39) Lee, M. J.; Lim, S. H.; Ha, J. M.; Choi, S. M. Green Synthesis of High-Purity Mesoporous Gold Sponges Using Self-Assembly of Gold Nanoparticles Induced by Thiolated Poly(ethylene glycol). *Langmuir* **2016**, *32*, 5937−5945.
(40) Roger, K.; Botet, R.; Cabane, B. Coalescence of Repelling Colloidal Droplets: A Route to Monodisperse Populations. *Langmuir* **2013**, *29*, 5689−5700.
(41) Fan, M.; Andrade, G. F. S.; Brolo, A. G. A Review on Recent Advances in the Applications of Surface-Enhanced Raman Scattering in Analytical Chemistry. *Anal. Chim. Acta* **2020**, *1097*, 1.
(42) Li, X.; Lenhart, J. J.; Walker, H. W. Aggregation kinetics and dissolution of coated silver nanoparticles. *Langmuir* **2012**, *28*, 1095−1104.
(43) Westley, C.; Xu, Y.; Carnell, A. J.; Turner, N. J.; Goodacre, R. Label-Free Surface Enhanced Raman Scattering Approach for High-Throughput Screening of Biocatalysts. *Anal. Chem.* **2016**, *88*, 5898−5903.
(44) Wen, P.; Yang, F.; Ge, C.; Li, S.; Xu, Y.; Chen, L. Self-assembled nano-Ag/Au@Au film composite SERS substrates show high uniformity and high enhancement factor for creatinine detection. *Nanotechnology* **2021**, *32*, 395502.
(45) Wang, C.; Shang, M.; Wei, H.; Zhang, M.; Zou, W.; Meng, X.; Chen, W.; Shao, H.; Lai, Y. Specific and sensitive on-site detection of Cr(VI) by surface-enhanced Raman spectroscopy. *Sens. Actuators, B* **2021**, *346*, 130594.
(46) Markina, N. E.; Markin, A. V.; Weber, K.; Popp, J.; Cialla-May, D. Liquid-liquid extraction-assisted SERS-based determination of sulfamethoxazole in spiked human urine. *Anal. Chim. Acta* **2020**, *1109*, 61−68.
(47) Aitekenov, S.; Sultangaziyev, A.; Abdirova, P.; Yussupova, L.; Gaipov, A.; Utegulov, Z.; Bukasov, R. *Raman, Infrared and Brillouin Spectroscopies of Biofluids for Medical Diagnostics and for Detection of Biomarkers*, 2022; Vol. *94*(11), pp 4850−4858.

https://doi.org/10.1021/acsomega.3c00005
ACS Omega 2023, 8, 12878−12885